On the Influence of Doubly-Selectivity in Pilot-Aided Channel Estimation for FBMC-OQAM

Ronald Nissel, Erich Zöchmann and Markus Rupp
Christian Doppler Laboratory for Dependable Wireless Connectivity for the Society in Motion,
Institute of Telecommunications, TU Wien, Vienna, Austria
Email: {rnissel, ezoechmann, mrupp}@nt.tuwien.ac.at

***Abstract*—Superior spectral properties of Filter Bank Multi-Carrier (FBMC) techniques make them an interesting choice for future wireless systems. In order to directly apply well-known pilot-symbol aided channel estimation in FBMC, however, the intrinsic imaginary interference has to be canceled. Such cancellation method is usually designed for a doubly-flat channel. In this paper, we investigate the effects of doubly-selectivity, that is, time-selectivity and frequency-selectivity, on the channel estimation Mean Squared Error (MSE) in FBMC. The calculation of the MSE is based on a compact matrix description, allowing us also to find an MSE minimizing channel estimation method that takes the underlying waveform into account.**

I. Introduction

Filter Bank Multi-Carrier (FBMC) with Offset Quadrature Amplitude Modulation (OQAM), in short just FBMC, has better spectral properties compared to legacy Orthogonal Frequency Division Multiplexing (OFDM). This allows a flexible assignment of the available time-frequency resources so that a large range of possible use cases can be efficiently supported. The improved spectral properties of FBMC, however, come at a price, namely, imaginary interference which makes certain techniques, such as Multiple-Input and Multiple-Output (MIMO) and channel estimation, more challenging. For MIMO, we have recently shown theoretically and through real world measurements that it can be efficiently combined with FBMC [1], [2]. Thus, one of the biggest issues has been resolved, making FBMC a viable choice for future wireless communication systems.

In this paper, we investigate channel estimation in FBMC. One possible method to estimate the channel is based on preambles [3], but we focus here on pilot-aided channel estimation [4] because it allows to track the channel in time and is therefore better suited for a future society in motion [5]. To deal with the imaginary interference at the pilot positions, we consider three different cancellation techniques: one auxiliary symbol [6], two auxiliary symbols [7] and coding [8].

While there exist many papers which investigate pilot-symbol aided channel estimation in OFDM from an analytical point of view [9], [10], most works on channel estimation for FBMC rely purely on simulations [6]–[8]. We therefore propose a novel matrix formulation to calculate closed-form solutions for the channel estimation Mean Squared Error (MSE) in FBMC transmissions over time and frequency selective channels. Furthermore, we derive an optimal interpolation method, that is, Minimum Mean Squared Error (MMSE), which, in contrast to previous works, takes also the underlying waveform into account.

After submission of this paper, a similar work [11] was accepted for publication. However, [11] does not compare to OFDM and employs only linear channel interpolation, while we derive the MMSE interpolation.

II. Multicarrier Modulation

Let us first consider a time-continuous representation of multicarrier systems because it describes the underlying idea best. Afterwards, we will reformulate the transmission system in discrete-time domain using a compact matrix description, simplifying analytical investigations. The transmitted signal $s(t)$, consisting of L subcarriers and K time-symbols, can be expressed by

$$s(t) = \sum_{k=1}^{K} \sum_{l=1}^{L} g_{l,k}(t)\, x_{l,k}, \tag{1}$$

where the data symbols $x_{l,k}$ at subcarrier-position l and time-position k are modulated by the transmit basis pulses $g_{l,k}(t)$, essentially, time and frequency shifted versions of the transmit prototype filter $p_{\text{TX}}(t)$:

$$g_{l,k}(t) = p_{\text{TX}}(t - kT)\, \mathrm{e}^{\mathrm{j}2\pi\, lF\,(t-kT)}\, \mathrm{e}^{\mathrm{j}\theta_{l,k}} \tag{2}$$

Note that time-spacing T and frequency-spacing F (subcarrier spacing) determine the spectral efficiency. The received symbols $y_{l,k}$ are then obtained by projecting the received signal $r(t)$ onto the receive basis pulses $q_{l,k}(t)$, that is,

$$y_{l,k} = \langle r(t), q_{l,k}(t) \rangle = \int_{-\infty}^{-\infty} r(t) q_{l,k}^{*}(t)\, \mathrm{d}t, \tag{3}$$

with

$$q_{l,k}(t) = p_{\text{RX}}(t - kT)\, \mathrm{e}^{\mathrm{j}2\pi\, lF\,(t-kT)}\, \mathrm{e}^{\mathrm{j}\theta_{l,k}}. \tag{4}$$

Desired properties of multicarrier systems are: (bi)-orthogonality: $\langle g_{l_1,k_1}(t), q_{l_2,k_2}(t) \rangle = \delta_{(l_1-l_2),(k_1-k_2)}$, time-localization, frequency-localization and maximum spectral efficiency ($TF = 1$). Unfortunately it is not possible to satisfy all of these properties at the same time according to the Balian-Low theorem. In pure OFDM (no Cyclic Prefix (CP)) the underlying rectangular function leads to a violation of frequency-localization. In FBMC, on the other hand, complex orthogonality is replaced by the less strict real orthogonality condition, making certain techniques more challenging. The idea behind FBMC is as follows: we design a pulse which is orthogonal for $TF = 2$, for example based

on Hermite polynomials [12]. Then, the time spacing as well as the frequency spacing is reduced by a factor of two, leading to $TF = 0.5$. This generates interference which, however, is shifted to the purely imaginary domain by the phase-shift $\theta_{l,k} = \frac{\pi}{2}(l+k)$. By taking the real part, we can completely eliminate this interference and are able to employ low complexity one-tap equalizers. Only real valued symbols can be transmitted in such a way so that we need two time-slots to transmit one complex-valued symbol. Thus, our time-frequency spacing of $TF = 0.5$ corresponds to $TF = 1$ in terms of complex valued symbols, leading to maximum spectral efficiency.

Let us now reformulate the transmission model in matrix notation: the sampled transmit signal $s(t)$ in (1) can be rewritten by

$$\mathbf{s} = \mathbf{G}\mathbf{x}, \tag{5}$$

with

$$\mathbf{G} = \begin{bmatrix} \mathbf{g}_{1,1} & \mathbf{g}_{2,1} & \cdots & \mathbf{g}_{L,1} & \mathbf{g}_{1,2} & \cdots & \mathbf{g}_{L,K} \end{bmatrix} \tag{6}$$

$$\mathbf{x} = \begin{bmatrix} x_{1,1} & x_{2,1} & \cdots & x_{L,1} & x_{1,2} & \cdots & x_{L,K} \end{bmatrix}^{\mathsf{T}}, \tag{7}$$

whereas $\mathbf{g}_{l,k} \in \mathbb{C}^{N\times 1}$ is obtained by sampling the basis pulses $g_{l,k}(t)$ in (2) and stacking these samples in a large vector. The variable N denotes the number of samples of the whole transmission block and not only the samples per multicarrier symbol! As in (5)-(7), we can reformulate the receive process in (3) by:

$$\mathbf{y} = \mathbf{Q}^{\mathsf{H}}\,\mathbf{r}, \tag{8}$$

with

$$\mathbf{y} = \begin{bmatrix} y_{1,1} & y_{2,1} & \cdots & y_{L,1} & y_{1,2} & \cdots & y_{L,K} \end{bmatrix}^{\mathsf{T}} \tag{9}$$

$$\mathbf{Q} = \begin{bmatrix} \mathbf{q}_{1,1} & \mathbf{q}_{2,1} & \cdots & \mathbf{q}_{L,1} & \mathbf{q}_{1,2} & \cdots & \mathbf{q}_{L,K} \end{bmatrix}. \tag{10}$$

Similar as before, $\mathbf{q}_{l,k} \in \mathbb{C}^{N\times 1}$ reflects the sampled basis pulses in (4). In an Additive White Gaussian Noise (AWGN) channel, the Signal-to-Noise Ratio (SNR) is maximized by a matched filter, $\mathbf{Q} = \mathbf{G}$. However, in CP-OFDM we employ a receive pulse which is shorter than the transmit pulse, $\mathbf{Q} \neq \mathbf{G}$, in order to gain robustness in a frequency selective channel. Note that the (bi)-orthogonality condition in OFDM implies that $\mathbf{Q}^{\mathsf{H}}\mathbf{G} = \mathbf{I}_{LK}$, while in FBMC we observe imaginary interference, and only $\Re\{\mathbf{Q}^{\mathsf{H}}\mathbf{G}\} = \mathbf{I}_{LK}$, with $\mathbf{Q} = \mathbf{G}$, holds.

The effect of time-variant multipath propagation can be modeled by a time-variant convolution matrix $\mathbf{H} \in \mathbb{C}^{N\times N}$, so that the overall transmission system becomes:

$$\mathbf{y} = \mathbf{Q}^{\mathsf{H}}\,\mathbf{H}\,\mathbf{G}\,\mathbf{x} + \mathbf{Q}^{\mathsf{H}}\mathbf{z}. \tag{11}$$

The statistical characterization of $\mathbf{H}$ is determined by the power delay profile and the Doppler spectral density, while $\mathbf{z} \sim \mathcal{CN}(\mathbf{0}, P_{\mathrm{z}}\,\mathbf{I}_{LK})$ represents the white Gaussian noise. The big advantage of multicarrier systems is that the main energy is usually concentrated at the diagonal elements of $\mathbf{Q}^{\mathsf{H}}\mathbf{H}\mathbf{G}$, so that low-complexity one-tap equalizers achieve good performances. The off-diagonal elements are then treated as interference, similar to noise. We can thus split (11) according to

$$y_{l,k} = \underbrace{\mathbf{q}_{l,k}^{\mathsf{H}}\,\mathbf{H}\,\mathbf{g}_{l,k}}_{h_{l,k}}\,x_{l,k} + \underbrace{\mathbf{q}_{l,k}^{\mathsf{H}}\mathbf{H}\,\mathbf{G}_{\text{-}(l,k)}\,\mathbf{x}}_{\text{Interference}} + n_{l,k}, \tag{12}$$

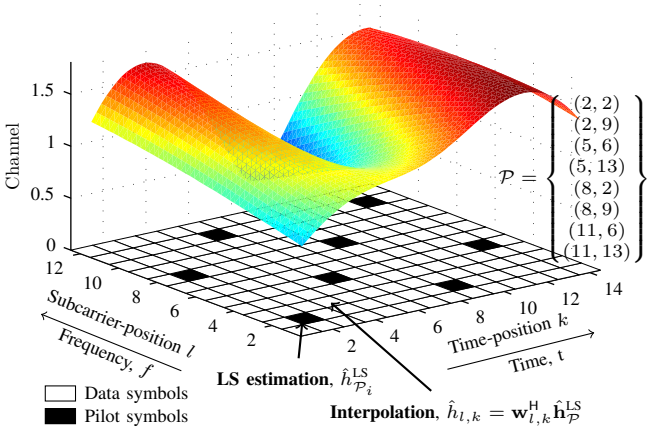

Fig. 1. Pilot-symbol aided channel estimation consists of two basic steps: Firstly, a LS channel estimation at the pilot positions. Secondly, interpolation of those LS estimates to obtain channel estimates at the data positions.

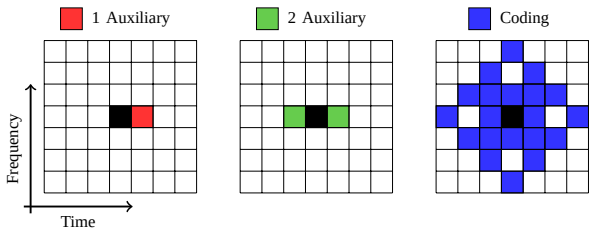

Fig. 2. In order to straightforwardly apply pilot symbol aided channel estimation in FBMC, we have to cancel the imaginary interference at the pilot positions. One auxiliary symbol wastes too much energy, two auxiliary symbols causes a further loss of data symbols and coding requires a higher computational complexity.

where $h_{l,k}$ describes the one-tap channel, corresponding to the appropriate diagonal element of $\mathbf{Q}^{\mathsf{H}}\mathbf{H}\mathbf{G}$ and $n_{l,k} \sim \mathcal{CN}(0, P_{\mathrm{n}})$ the Gaussian noise with $P_{\mathrm{n}} = P_{\mathrm{z}}\,\mathbf{q}_{l,k}^{\mathsf{H}}\mathbf{q}_{l,k}$. Matrix $\mathbf{G}_{\text{-}(l,k)}$ in (12) reflects the interference and consists of almost the same elements as $\mathbf{G}$ in (6), except that the basis pulse vector $\mathbf{g}_{l,k}$ becomes an all zero vector $\mathbf{0}$, that is,

$$\left[\mathbf{G}_{\text{-}(l,k)}\right]_{i,j} = \begin{cases} 0 & j = l + L(k-1) \\ [\mathbf{G}]_{i,j} & \text{otherwise} \end{cases}. \tag{13}$$

The ultimate goal at the receiver is to estimate the transmitted data symbols $x_{l,k}$ which can be accomplished by a one-tap equalizer, that is, $\frac{y_{l,k}}{h_{l,k}}$. As long as the interference is dominated by the noise, such one-tap equalizers achieve good performances and even correspond to the maximum likelihood symbol detection (Gaussian noise). Note that in FBMC, the interference term in (12) remains even in an AWGN channel ($\mathbf{H} = \mathbf{I}_N$) but becomes purely imaginary, so that, by taking the real part, we completely eliminate this interference which is the key idea behind FBMC.

III. Pilot-Symbol Aided Channel Estimation

In order to apply one-tap equalization in practice, we first need an accurate estimate of the channel $\hat{h}_{l,k}$, accomplished in this paper by pilot-symbol aided channel estimation. The idea is illustrated in Figure 1: the so called pilot symbols, $x_{l,k}$ for $(l,k) \in \mathcal{P}$, are known a-priori at the receiver and are used

to estimate the channel. By utilizing (12) we obtain a Least Squares (LS) channel estimation at the pilot positions:

$$\hat{h}^{\mathrm{LS}}_{\mathcal{P}_i} = \frac{y_{\mathcal{P}_i}}{x_{\mathcal{P}_i}}, \tag{14}$$

where $\mathcal{P}_i$ corresponds to the i-th pilot position, see Figure 1. The channel at the data positions can then be estimated through interpolation, that is,

$$\hat{h}_{l,k} = \mathbf{w}^{\mathsf{H}}_{l,k} \hat{\mathbf{h}}^{\mathrm{LS}}_{\mathcal{P}}, \tag{15}$$

where we stack all LS estimates from (14) in the vector $\hat{\mathbf{h}}^{\mathrm{LS}}_{\mathcal{P}} \in \mathbb{C}^{|\mathcal{P}|\times 1}$. The vector function $\mathbf{w}_{l,k} \in \mathbb{C}^{|\mathcal{P}|\times 1}$ describes an arbitrary interpolation method, for example, nearest neighbor, linear, spline or (linear) MMSE interpolation (the interference is approximately Gaussian distributed, so that the linear MMSE estimation corresponds to the MMSE solution).

Channel Estimation in FBMC

In OFDM the channel estimation process works exactly as described in (14) and (15). In FBMC, however, the LS channel estimation at the pilot position becomes more challenging: FBMC is based on the idea of taking the real part in order to get rid of the imaginary interference, which only works after channel (phase) equalization, not possible prior the channel estimation. We thus have to operate in the complex domain where we observe a Signal-to-Interference Ratio (SIR) of 0 dB, too low for accurate channel estimations. To circumvent this problem, we modify the transmitted symbols close to the pilot position so that they cancel the imaginary interference at the pilot positions. The unit-power data symbols $\tilde{\mathbf{x}}$ are precoded by $\mathbf{C}$, so that the transmitted symbols transform to

$$\mathbf{x} = \mathbf{C}\,\tilde{\mathbf{x}}, \tag{16}$$

whereas the precoding should not change the transmit power, that is, $\mathrm{tr}\{\mathbf{C}\mathbf{C}^{\mathsf{H}}\} = LK$. Usually, channel state information is not available at the transmitter, so that $\mathbf{C}$ is designed to cancel the imaginary interference for the assumption of a flat channel. This is similar to the design of the basis pulses in (2) and (4) for which the (real) orthogonality condition also only holds in a flat channel. The cancellation condition can then be expressed as:

$$\mathbf{q}^{\mathsf{H}}_{\mathcal{P}_i}\, \mathbf{G}_{\text{-}\mathcal{P}_i} \mathbf{C}\, \tilde{\mathbf{x}} = 0, \tag{17}$$

where we use the same notation as in (12) and (13) but now $\mathcal{P}_i$ denotes the position (l,k) which corresponds to the i-th pilot symbol. There exist different methods satisfying (17), see Figure 2. One auxiliary symbol per pilot, the classical approach [6], has the drawback of a large auxiliary-symbol power-offset. Employing two auxiliary symbols reduces this power-offset, at the additional cost of one (real-valued) data symbol. However, the saved power outweighs the loss of one data symbol for small to medium SNR ranges, so that the overall throughput increases [7]. For a flat-fading channel, coding achieves the best performance of all those cancellation techniques because no power is wasted [12]: Here, we spread $M-1$ data symbols over M time-frequency positions and utilize the additional degree of freedom to cancel the imaginary interference. This method, however, needs de-spreading at the receiver which increases the computational complexity.

IV. Mean Squared Error

Let us now calculate the MSE of the channel estimation methods described in Section III. Following the basic steps of pilot-symbol aided channel estimation, we first investigate the LS estimation at the pilot positions and then shift our attention to interpolation.

A. LS Channel Estimation

Inserting (12) into (14) allows us to express the LS channel estimation error at the i-th pilot position by:

$$\hat{h}^{\mathrm{LS}}_{\mathcal{P}_i} - h_{\mathcal{P}_i} = \mathbf{q}^{\mathsf{H}}_{\mathcal{P}_i} \mathbf{H}\, \mathbf{G}_{\text{-}\mathcal{P}_i} \mathbf{C}\, \frac{\tilde{\mathbf{x}}}{x_{\mathcal{P}_i}} + \frac{n_{\mathcal{P}_i}}{x_{\mathcal{P}_i}} \tag{18}$$

$$= \left(\left(\mathbf{G}_{\text{-}\mathcal{P}_i} \mathbf{C}\, \frac{\tilde{\mathbf{x}}}{x_{\mathcal{P}_i}} \right)^{\mathsf{T}} \otimes \mathbf{q}^{\mathsf{H}}_{\mathcal{P}_i} \right) \mathrm{vec}\{\mathbf{H}\} + \frac{n_{\mathcal{P}_i}}{x_{\mathcal{P}_i}}, \tag{19}$$

whereas we use the Kronecker product $\otimes$ to rewrite (18) by (19) which greatly simplifies statistical investigations. Indeed, the MSE can be straightforwardly calculated by:

$$\mathrm{MSE}^{\mathrm{LS}}_{\mathcal{P}_i} = \mathbb{E}\left\{ |h_{\mathcal{P}_i} - \hat{h}^{\mathrm{LS}}_{\mathcal{P}_i}|^2 \right\} = \tag{20}$$

$$\frac{1}{\kappa} \mathrm{tr}\Big\{ \big((\mathbf{G}_{\text{-}\mathcal{P}_i} \mathbf{C})^{\mathsf{T}} \otimes \mathbf{q}^{\mathsf{H}}_{\mathcal{P}_i} \big) \mathbf{R}_{\mathrm{vec}\{\mathbf{H}\}} \big((\mathbf{G}_{\text{-}\mathcal{P}_i} \mathbf{C})^{\mathsf{T}} \otimes \mathbf{q}^{\mathsf{H}}_{\mathcal{P}_i} \big)^{\mathsf{H}} \Big\} + \frac{P_{\mathrm{n}}}{\kappa}, \tag{21}$$

where $\kappa = \mathbb{E}\{|x_{\mathcal{P}_i}|^2\}$ denotes the power of the pilot symbols (all pilots have the same magnitude) and $\mathbf{R}_{\mathrm{vec}\{\mathbf{H}\}} = \mathbb{E}\{\mathrm{vec}\{\mathbf{H}\}\mathrm{vec}\{\mathbf{H}\}^{\mathsf{H}}\} \in \mathbb{C}^{N^2\times N^2}$ the sparse correlation matrix of the vectorized time-variant convolution matrix. Note that (21) covers also the case of OFDM if $\mathbf{C} = \mathbf{I}_{LK}$. The (complex) noise power P_{n} is two times higher in FBMC compared to OFDM. After taking the real part, however, we end up with the same SNR. Imaginary interference cancellation based on coding saves power due to the spreading which can then be put into the pilot symbol power $\kappa = 2$, leading to the same data transmission SNR and channel estimation SNR. Auxiliary symbols, on the other hand, waste energy, so that κ is slightly smaller than 2.

B. Interpolation

The channel estimation at arbitrary position (l,k) is obtained through interpolation, see (15). Its MSE can be calculated similar to (18)-(21), leading to:

$$\mathrm{MSE}_{l,k} = \mathbb{E}\left\{ |h_{l,k} - \mathbf{w}^{\mathsf{H}}_{l,k} \hat{\mathbf{h}}^{\mathrm{LS}}_{\mathcal{P}}|^2 \right\} \tag{22}$$

$$= (\mathbf{a}_{l,k} - \mathbf{w}^{\mathsf{H}}_{l,k}\mathbf{B})\, \mathbf{R}_{\mathrm{vec}\{\mathbf{H}\}}\, (\mathbf{a}_{l,k} - \mathbf{w}^{\mathsf{H}}_{l,k}\mathbf{B})^{\mathsf{H}} + \\ + \mathbf{w}^{\mathsf{H}}_{l,k}\, \mathrm{diag}\{\mathbf{MSE}^{\mathrm{LS}}_{\mathcal{P}}\}\, \mathbf{w}_{l,k}, \tag{23}$$

whereas the vector $\mathbf{a}_{l,k} \in \mathbb{C}^{1\times N^2}$ and the matrix $\mathbf{B} \in \mathbb{C}^{|\mathcal{P}|\times N^2}$ help to keep the notation compact and are defined as:

$$\mathbf{a}_{l,k} = \mathbf{g}^{\mathsf{T}}_{l,k} \otimes \mathbf{q}^{\mathsf{H}}_{l,k} \quad \text{and} \quad \mathbf{B} = \begin{bmatrix} \mathbf{g}^{\mathsf{T}}_{\mathcal{P}_1} \otimes \mathbf{q}^{\mathsf{H}}_{\mathcal{P}_1} \\ \vdots \\ \mathbf{g}^{\mathsf{T}}_{\mathcal{P}_{|\mathcal{P}|}} \otimes \mathbf{q}^{\mathsf{H}}_{\mathcal{P}_{|\mathcal{P}|}} \end{bmatrix}. \tag{24}$$

Furthermore, the vector $\mathbf{MSE}^{\mathrm{LS}}_{\mathcal{P}} \in \mathbb{R}^{|\mathcal{P}|\times 1}$ in (23) stacks all MSE values from (20) in a vector. Note that the division by the pilot symbols in (14) makes the LS channel estimation error uncorrelated to all other variables. In particular, we are

able to employ the diagonal operator $\mathrm{diag}\{\cdot\}$ in (23) without considering any cross correlations. Having calculated the MSE in (23), a natural question is which interpolation method $\mathbf{w}_{l,k}$ minimizes the MSE. By utilizing the orthogonal projection theorem, that is, $\mathbb{E}\{(h_{l,k}-\hat{h}_{l,k})\hat{h}^*_{l,k}\}=0$, we find such MSE minimizing interpolation vector by

$$\mathbf{w}^{\mathrm{MMSE}}_{l,k} = \arg\min_{\mathbf{w}_{l,k}} \mathbb{E}\left\{|h_{l,k}-\mathbf{w}^{\mathsf{H}}_{l,k}\hat{\mathbf{h}}^{\mathrm{LS}}_{\mathcal{P}}|^2\right\} \tag{25}$$

$$= \left(\mathbf{B}\,\mathbf{R}_{\mathrm{vec}\{\mathbf{H}\}}\,\mathbf{B}^{\mathsf{H}} + \mathrm{diag}\{\mathbf{MSE}^{\mathrm{LS}}_{\mathcal{P}}\}\right)^{-1}\mathbf{B}\,\mathbf{R}_{\mathrm{vec}\{\mathbf{H}\}}\,\mathbf{a}^{\mathsf{H}}_{l,k}. \tag{26}$$

Not surprising, the structure of (26) follows closely conventional MMSE solutions, see for example [9]. However, usually the correlations $\mathbb{E}\{h_{l_1,k_1}h^*_{l_2,k_2}\}$ are assumed to be known. We, on the other hand, show in (26) how the basis pulses, see (2) and (4), determine these correlation matrices, that is, $\mathbf{R}_{\mathbf{h}_{\mathcal{P}}}=\mathbf{B}\,\mathbf{R}_{\mathrm{vec}\{\mathbf{H}\}}\,\mathbf{B}^{\mathsf{H}}$ and $\mathbf{R}_{\mathbf{h}_{\mathcal{P}},h_{l,k}}=\mathbf{B}\,\mathbf{R}_{\mathrm{vec}\{\mathbf{H}\}}\,\mathbf{a}^{\mathsf{H}}_{l,k}$.

V. Numerical Results

In this section we validate our analytical MSE calculations in (21) and (23) by simulations, assuming a Jakes Doppler spectrum. The subcarrier spacing is set to 15 kHz, same as in LTE. We compare OFDM without CP, OFDM with CP (4.7 μs, same as in LTE) and FBMC-OQAM based on a Hermite prototype filter [12]. In a time-variant channel, such Hermite prototype filter performs better than the often considered PHYDYAS prototype filter [13]. To better investigate the effect of a doubly-selective channel, we set the noise power P_{n} to zero. This is feasible for the LS estimation because interference and noise can be separated, as shown in (20), where we see that the noise power is only an additive term. Thus, in order to determine the MSE including noise, we only have to add the noise power to the MSE without noise. Figure 3 shows the MSE at the pilot-positions, see (21), over velocity for a Pedestrian A channel model (10.08 MHz sampling frequency). In general, FBMC performs better than OFDM because FBMC is more robust in a time-variant channel due to better joint time-frequency localization. It turns out that the cancellation condition in (17), designed for a doubly-flat channel, works well in doubly-selective channels. Only FBMC based on one auxiliary symbol per pilot performs poorly (close to OFDM) because the large power-offset of the auxiliary symbol leads to a relatively strong interference. The method based on two auxiliary symbols per pilot, on the other hand, has a reduced power-offset, leading to less interference and therefore to a much better MSE. However, we have to keep in mind that one additional real data symbol is required compared to OFDM without CP and FBMC based on one auxiliary symbol and coding. Note that there is little difference between OFDM with and without CP because the Root Mean Square (RMS) delay spread is relatively small (46 ns). Figure 4 plots the MSE for a Vehicular A channel model (2.94 MHz sampling frequency). Compared to Pedestrian A, we have a higher RMS delay spread (370 ns), so that, for low velocities, we see a deviation between these two figures. For higher velocities, on the other hand, the interference is dominated by the Doppler spread so

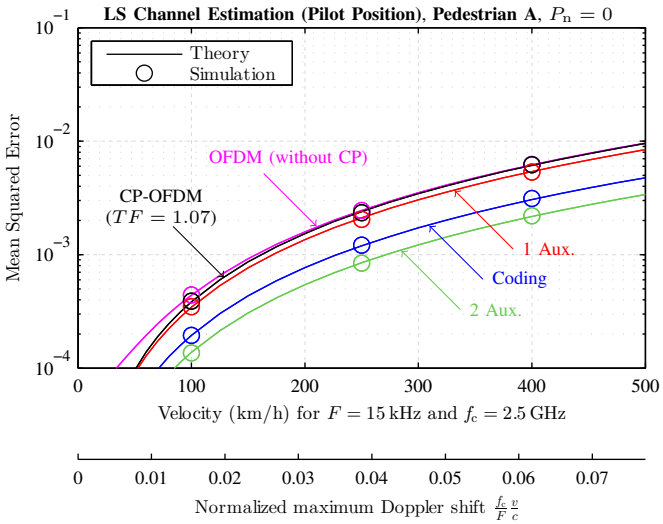

Fig. 3. FBMC (1 Aux, 2 Aux and Coding) performs better than OFDM due to better joint time-frequency localization and the fact that the imaginary interference cancellation method is advantageous in some cases. Two auxiliary symbols perform best but one additional data symbol has to be sacrificed for each pilot. Coding is slightly worse but has the advantage of not wasting any power and having the same pilot overhead as OFDM without CP.

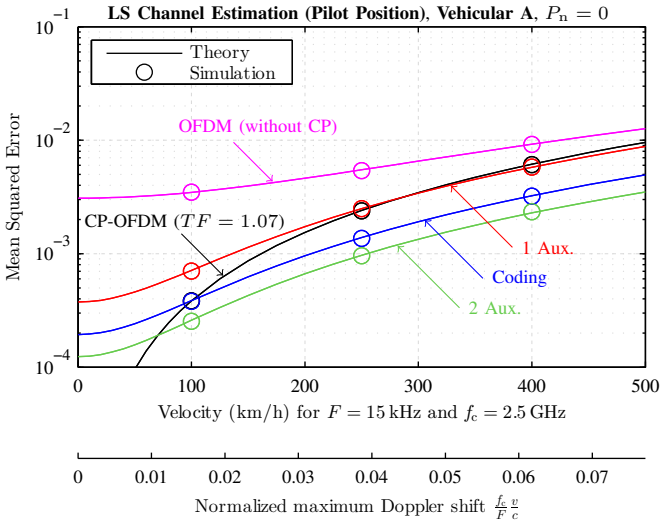

Fig. 4. The Vehicular A channel model has a higher RMS delay spread compared to the Pedestrian A channel model, so that we observe differences for small velocities.

that they have a similar MSE. For low velocities, OFDM with CP performs best because the CP guarantees orthogonality as long as the maximum channel delay is smaller than the CP length. However, this comes at the price of reduced spectral efficiency ($TF=1.07$). Furthermore, the advantage of CP-OFDM compared to FBMC soon vanishes for higher velocities because FBMC is more robust in a time-variant channel.

In order to investigate the effect of interpolation on the MSE, we assume $L=12$ subcarriers and, for OFDM without CP, $K=15$ symbols, for OFDM with CP $K=14$ symbols and for FBMC $K=30$ symbols. This results in the same transmission time $KT=1$ ms for all these techniques. Similar as in LTE, we chose a diamond-shaped pilot pattern

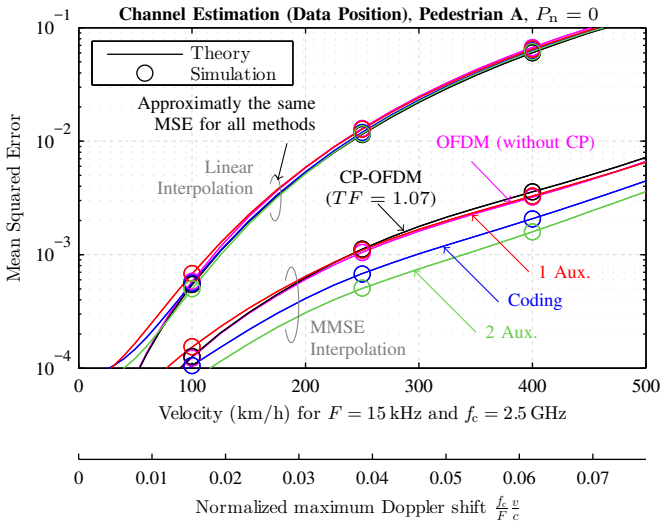

Fig. 5. The interpolation method plays an imporant role. In particular, linear interpolation (a straight line) performs poorly so that the advantages of FBMC are not translated to the channel estimation because the interpolation error dominates the MSE.

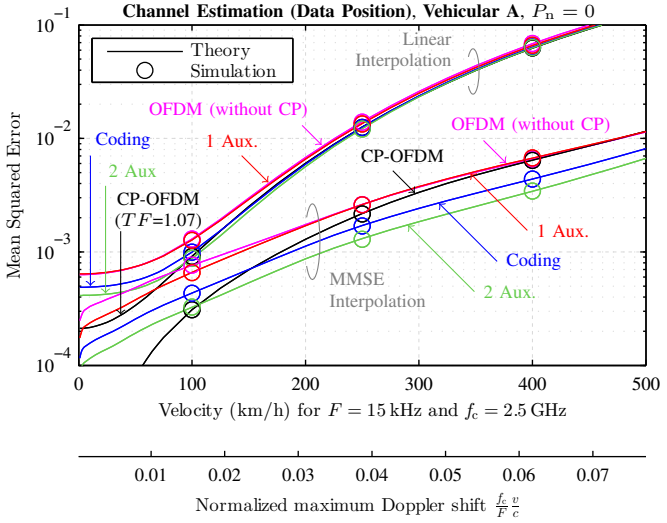

Fig. 6. For low velocities, the RMS delay spread limits the system performance (except for CP-OFDM). However, a MSE of -40 dB. . . -35 dB is good enough for most practical use cases.

and a pilot density of $|\mathcal{P}|/(KTFL) = 0.044$ which, for a fair comparison, is also the same for all methods. For a Pedestrian A channel model, Figure 5 shows the channel estimation MSE at the data positions, see (23). We see that a simple interpolation method, for example linear interpolation (a straight line), leads to a poor MSE. The interpolation error dominates any advantages of a better LS channel estimate, so that all methods show approximately the same performance. By employing a better interpolation method such as MMSE interpolation (the best possible technique in terms of MSE), we see that the superior LS estimation of FBMC translates also into a better performance of the channel estimates at the data positions. The MSE is then even better than for the LS estimates at the pilot positions because we utilize the correlation of eight pilots, improving the estimation accuracy. Figure 6 shows the case of a Vehicular A channel model. Similar as for the LS channel estimation, we see the effects of a high RMS delay spread for low velocities in the MSE. Additionally, a high delay spread also leads to a small channel correlation in the frequency domain, decreasing the estimation accuracy further.

Due to lack of space, we will not include Bit Error Ratio (BER) simulations in this paper. However, it is worth mentioning that all the results we observe for the MSE also translate to the BER [14].

VI. Conclusion

Although the imaginary interference cancellation condition at the pilot-positions in FBMC is designed for a doubly-flat channel, we observe in many cases a more accurate channel estimate than in OFDM. However, if the interpolation method is chosen poorly, this error dominates any potential improvement of a better LS estimate at the pilot positions, so that all modulation methods perform similar.

Acknowledgment The financial support by the Austrian Federal Ministry of Science, Research and Economy, the National Foundation for Research, Technology and Development, and the TU Wien is gratefully acknowledged.

References

[1] R. Nissel and M. Rupp, "Enabling low-complexity MIMO in FBMC-OQAM," in *IEEE Globecom Workshops (GC Wkshps)*, Washington, USA, Dec 2016.

[2] R. Nissel, E. Zöchmann, M. Lerch, S. Caban, and M. Rupp, "Low-latency MISO FBMC-OQAM: It works for millimeter waves!" in *IEEE International Microwave Symposium*, Honolulu, Hawaii, June 2017.

[3] C. Lélé, J.-P. Javaudin, R. Legouable, A. Skrzypczak, and P. Siohan, "Channel estimation methods for preamble-based OFDM/OQAM modulations," *Europ. Trans. on Telecom.*, vol. 19, no. 7, pp. 741–750, 2008.

[4] R. Nissel and M. Rupp, "Bit error probability for pilot-symbol aided channel estimation in FBMC-OQAM," in *IEEE International Conference on Communications (ICC)*, Kuala Lumpur, Malaysia, May 2016.

[5] S. Schwarz and M. Rupp, "Society in motion: Challenges for LTE and beyond mobile communications," *IEEE Commun. Mag., Feature Topic: LTE Evolution*, vol. 54, no. 5, 2016.

[6] J.-P. Javaudin, D. Lacroix, and A. Rouxel, "Pilot-aided channel estimation for OFDM/OQAM," in *IEEE Vehicular Technology Conference (VTC)*, vol. 3, 2003, pp. 1581–1585.

[7] R. Nissel, S. Caban, and M. Rupp, "Experimental evaluation of FBMC-OQAM channel estimation based on multiple auxiliary symbols," in *IEEE Sensor Array and Multichannel Signal Processing Workshop (SAM)*, Rio de Janeiro, Brazil, July 2016.

[8] C. Lélé, R. Legouable, and P. Siohan, "Channel estimation with scattered pilots in OFDM/OQAM," in *IEEE Workshop on Signal Processing Advances in Wireless Communications (SPAWC)*, 2008, pp. 286–290.

[9] H. Arslan *et al.*, "Channel estimation for wireless OFDM systems," *IEEE Surveys and Tutorials*, vol. 9, no. 2, pp. 18–48, 2007.

[10] P. Hoeher, S. Kaiser, and P. Robertson, "Two-dimensional pilot-symbol-aided channel estimation by Wiener filtering," in *IEEE International Conference on Acoustics, Speech and Signal Processing (ICASSP)*, 1997.

[11] M. Fuhrwerk, S. Moghaddamnia, and J. Peissig, "Scattered pilot based channel estimation for channel adaptive FBMC-OQAM systems," *IEEE Trans. Wireless Commun.*, 2017, accepted for publication.

[12] R. Nissel and M. Rupp, "On pilot-symbol aided channel estimation in FBMC-OQAM," in *IEEE International Conference on Acoustics, Speech and Signal Processing (ICASSP)*, Shanghai, China, March 2016.

[13] M. Bellanger, D. Le Ruyet, D. Roviras, M. Terré, J. Nossek, L. Baltar, Q. Bai, D. Waldhauser, M. Renfors, T. Ihalainen *et al.*, "FBMC physical layer: a primer," *PHYDYAS, January*, 2010.

[14] R. Nissel and M. Rupp, "OFDM and FBMC-OQAM in doubly-selective channels: Calculating the bit error probability," *IEEE Communications Letters*, 2017, accepted for publication.